

Analysis of the Gas Phase Kinetics Active during GaN Deposition from NH_3 and $\text{Ga}(\text{CH}_3)_3$

Stefano Ravasio,[†] Takeshi Momose,[‡] Katsushi Fujii,[§] Yukihiro Shimogaki,[‡] Masakazu Sugiyama,[§] and Carlo Cavallotti^{*,†}

[†]Dipartimento di Chimica, Materiali e Ingegneria Chimica "Giulio Natta", Politecnico di Milano, via Mancinelli 7, 20131 Milano, Italy

[‡]Department of Materials Engineering, The University of Tokyo, Bunkyo-ku, Tokyo 113-8656, Japan

[§]School of Engineering, The University of Tokyo, Bunkyo-ku, Tokyo 113-8656, Japan

Special Issue: 100 Years of Combustion Kinetics at Argonne: A Festschrift for Lawrence B. Harding, Joe V. Michael, and Albert F. Wagner

Received: February 11, 2015

Revised: April 21, 2015

Published: April 28, 2015

1. INTRODUCTION

The growth of high quality GaN thin solid films attracts great interest because of the several applications that are possible in optoelectronics, high power, and high frequency devices. The preferred industrial method to produce such material is metal organic vapor phase epitaxy (MOVPE), using ammonia and trimethyl gallium (TMGa) as gaseous precursors.¹ At the typical operative conditions for the GaN growth, it is generally agreed that the deposition rate is controlled by the diffusion of the growth precursors,^{2–7} because at the elevated temperatures (1200–1400 K) at which GaN is deposited surface reactions are generally fast. The gas phase kinetics active during GaN deposition plays an important role as it is responsible for producing the precursors to the GaN growth, as well as because its control is necessary in order to limit the formation of powders.^{1,3–12} This side reactivity is strongly undesired because these powders scavenge part of the precursors, limiting the deposition rate. Also, if they reach and get adsorbed on the

substrate, they can considerably affect the quality of the film, because of the inclusion of additional defects to the crystalline layer and as they can lead to deposition outside of the desired growth areas.

Several theoretical and experimental studies have been dedicated to investigate the GaN gas phase and surface growth kinetics.^{2–4,13–24} It is thus generally agreed that $\text{Ga}(\text{CH}_3)_3$ gas phase decomposition to GaCH_3 is competitive with several reactions with ammonia that eventually lead both to the production of the direct deposition precursor and of the critical nuclei, whose successive growth leads to the formation of GaN

powders. Several kinetic schemes have been proposed in the literature with the intent of describing the GaN growth mechanism. They can be differentiated on the basis of the precursors that are assumed to be formed before the deposition of the thin solid film and that lead to the formation of powders. The first mechanism was proposed by Mihopoulos et al.² and assumed that the TMGa and ammonia reacted in the gas phase to form TMGa:NH₃ acid–base adducts, whose decomposition would lead to the formation of the Ga(CH₃)_x(NH₂)_{3-x} species. Such species can then either adsorb and decompose on the surface to form the GaN film or associate in the gas phase to form dimers and trimers, which would then lead to the formation of powders. This mechanism was supported by experimental evidence, indicating that TMGa and NH₃ form adducts in the gas phase at low temperatures.^{13,25–27} Successive experimental studies performed by Bergmann et al.¹⁴ and Schafer et al.¹⁵ coupling molecular beam sampling and mass spectrometry, however, showed that the TMGa:NH₃ adduct decomposes rapidly as the temperature is increased so that it is unlikely that it may be the precursor to the film growth. In particular, these studies highlighted that as the temperature is increased, TMGa and ammonia react to form Ga(CH₃)₂NH₂, which was found as a dimer and, quite interestingly, a covalent molecule containing two Ga atoms covalently bound by an NH group: Ga₂NH(CH₃)₄. These species have maximum concentrations at around 700 K, though their signals drop at higher temperatures. Glockling and Strafford²⁸ also detected the trimeric compound Ga₃(CH₃)₉, though this finding was not confirmed in later studies. It is also interesting to report that it was experimentally found that at low gas phase temperatures the TMGa:NH₃ adduct is able to coordinate a second NH₃ molecule.²⁷ Unfortunately, while much is known of the reactivity of this system at low temperatures, it is still not clear what happens at substrate temperatures above 1000 K, which are the typical operative conditions of the process. The only experimental measurement at temperatures higher than 1000 K was performed by Schafer et al.,¹⁵ who found that in these conditions the main gas phase species becomes atomic Ga. This lead the authors to conclude that atomic Ga is the most likely growth precursor to GaN deposition.

The experimental uncertainty concerning the composition of the gas phase above the substrate during GaN deposition fostered a considerable theoretical effort, which exploited mostly DFT calculations in order to determine rate constants that could be used to investigate the gas phase kinetics active during GaN growth.^{2,16–19,22–24,29–33} Nowadays the kinetic mechanism most commonly adopted to model the gas phase kinetics of GaN MOVPE was proposed by Hirako et al.¹⁸ The proposed mechanism combines reactions proposed by several authors with kinetic constants evaluated using DFT methods. According to this mechanism, the main gas phase precursor to GaN deposition is the GaN diatomic molecule, formed from the decomposition of Ga(CH₃)₂NH₂ through the successive loss of two methane molecules. This mechanism, or similar mechanisms based on the formation of biatomic GaN as an intermediate, was used by several authors to model the deposition of GaN with success.^{3,4} The mechanism proposed by Hirako et al. also assumes that GaN powders are grown through successive addition of GaN species to a Ga₂N₂ nuclei formed by the addition of two GaN species. An alternative GaN gas phase mechanism was proposed by our group about one decade ago.^{17,21} It is based on the idea that a set of radical reactions may promote the decomposition of the reactants and

lead to the formation, as the most stable species at high temperature and therefore as growth precursor, of GaNH₂.

Summarizing, there is still at present considerable uncertainty about which is the growth precursor to GaN deposition as well as about the mechanism of formation of GaN powders in the gas phase. It is our opinion that these uncertainties are due at least in part to the lack of a thermodynamic database, which may be coupled to the gas phase mechanism in the modeling of the film deposition process and that may be used to determine which are the most stable gas phase species as a function of the operating conditions. Also, it is our opinion that several reaction pathways may have been neglected in previous works. The aims of the present study are the following: (i) compile a thermodynamic database that includes the most important gas phase GaN species; (ii) develop a kinetic mechanism that may be used to describe the gas phase reactivity and identify the main reaction routes; (iii) couple the gas phase mechanism to a surface mechanism and validate the kinetic mechanism through comparison with experimental growth rate data measured in well-defined operative conditions; (iv) develop a powder nucleation model that may be coupled to the reactor model. The present paper deals with points (i) and (ii), while the validation of the model through comparison with experimental data and the powder nucleation model will be presented in a successive work.

2. METHOD

The thermodynamic data of all the species considered in the equilibrium calculations were evaluated on the basis of energies, structures, and vibrational frequencies determined through ab initio simulations. In particular, formation enthalpies were determined at 298 K from atomization energies using as reference the experimental formation enthalpy of the elements, which were taken from the NIST-JANAF thermochemical tables.³⁴ Entropies were computed from translational, rotational, vibrational, and electronic partition functions using the rigid rotor-harmonic oscillator approximation and statistical thermodynamics. The same level of theory was also adopted to calculate the kinetic constants of all the gas phase reactions here studied, using conventional transition state theory. It is important to point out that the kinetic constants of reactions taken from previous papers were re-evaluated, with the exception of reactions whose rate constants are well established. This was done in order to avoid comparing reaction pathways using kinetic constants calculated at different levels of theory, as the different level of uncertainties may affect the comparison between the reaction pathways. The structures and the vibrational frequencies of all the stationary points were determined using density functional theory at the M062X/6-311+G(d,p) level.³⁵ In our experience,^{36–38} this approach allows predicting kinetic constants at a good level of approximation if combined with a high level estimation of the energy. For this purpose the energies of all the stationary points were determined at the ROCBS-QB3 level.³⁹ The kinetic constants here calculated can be considered to be more accurate with respect to those reported in previous works on the same system, because of the higher level at which energies and structures were computed. To validate the approach, some selected reaction energies were also evaluated at the CCSD-(T)/aug-cc-pVTZ level,⁴⁰ which is expected to be quite accurate for the system under investigation. In general, activation energies calculated at the two levels of theories differed by a maximum of about 1 kcal/mol, suggesting that the

adopted approach is reasonably accurate. In addition, in the present work we accounted for the degeneration of torsional vibrations into unhindered rotors, which considerably improves the evaluation of the density of states of reactants and transition states, and thus of rate constants and entropies.

For some reactions the minimum energy pathway does not present a saddle point. Therefore, their transition state was determined using canonical variational transitional state theory. The reaction path was scanned through constrained energy minimizations along the length of the breaking bond with the unrestricted M062X functional and the 6-311+G(d,p) basis set, thus allowing the partial occupation of the LUMO orbital. The potential energy surface (PES) so determined was then rescaled over reaction energies evaluated at the ROCBS-QB3 level. When relevant the low vibrational frequency associated with torsional motions was replaced by a 1D unhindered rotor model. This approximation is justified by the fact that such internal motions are mainly related to Ga-CH₃ bonds whose rotational PESs are characterized by hindrance potentials lower than 1 kcal/mol, as here verified with several tests on different molecules. The corresponding partition function was in this case determined using quantum eigenvalues, calculated as described in previous works.^{41,42} When two conversion channels with comparable rates were possible, global reaction rates were computed as the sum of the rates of the two channels. All calculations were performed using the Gaussian 09 computational suite.⁴³ The kinetic constants and the heat capacities so determined were then fitted to the modified Arrhenius form over a temperature range comprised between 500 and 1500 K.

A kinetic analysis was performed in order to determine which are the main reaction pathways active in the typical operative conditions of GaN MOVPE. For this purpose the gas phase kinetic mechanism was embedded in a fluid dynamic model of an experimental single wafer horizontal reactor (AIX200/4-RFS, AIXTRON). Specifically, simulations were performed using a stationary 2D CVD simulation code developed by Jensen and co-workers and already tested in several previous works, which also takes into account the surface reactivity.⁴⁴⁻⁵¹ Mass, momentum, and energy balance equations were integrated over a mesh consisting of about 4500 rectangular elements. The numerical solution is computed with the finite element method (FEM) using an analytical Jacobian. The model was used to evaluate the effect of a variation of some key rate constants on the gas phase composition and on the GaN growth rate, which allowed us to identify the main reaction routes.

3. RESULTS AND DISCUSSION

This section is organized in four parts. In the first one, the results of the thermodynamic analysis are reported. In the second, the reactions and rate constants included in the kinetic scheme are discussed. The third part is devoted to an analysis of the kinetic mechanism, aimed at clarifying which is the dominant reaction route. Finally, in the last part, other elementary reactions are initially considered, but then eliminated from the kinetic mechanism because it is found that they do not significantly affect the global reactivity, as described.

3.1. Thermodynamic Analysis. In order to perform a thermodynamic analysis, it is necessary to select a list of chemical species that are likely to be formed in the investigated conditions of temperature, pressure, and composition. The

initial list of considered compounds was selected on the basis of a literature research, focusing on the experimental^{14,15,20} and theoretical works¹⁶⁻¹⁹ that were performed to investigate the reaction kinetics of the GaN MOVPE. This list was then extended in order to account for other chemical species whose stability could be inferred from preliminary equilibrium calculations. For example, while Ga(CH₃)₂NH₂ was detected experimentally in several studies^{14,15} and was therefore included in the set of considered compounds, this was not the case for Ga(NH₂)₃, which was, however, considered after it became apparent that the substitution of methyl with amino groups is thermodynamically favored in the considered experimental conditions. The same consideration applies also to the logic that was followed to build the kinetic mechanism. On this basis, the following 32 chemical species were considered in the thermodynamic calculations: Ga(CH₃)₃, Ga(CH₃)₂NH₂, GaCH₃(NH₂)₂, Ga(NH₂)₃, Ga(CH₃)₂H, GaCH₃H₂, GaH, GaH(NH₂)₂, GaH₂NH₂, GaCH₃HNNH₂, GaCH₃, GaNH₂, GaH, Ga(NH₂)₂NH, GaCH₃NH₂NH, GaN, Ga, Ga₂NH(CH₃)₄, Ga₂NH(CH₃)₂(NH₂)₂, Ga₂NHCH₃(NH₂)₃, Ga₂NH(NH₂)₄, Ga₂NHH(NH₂)₃, Ga₂NHCH₃H(NH₂)₂, Ga₂NHH₂(NH₂)₂, Ga₃(NH)₃H₃, Ga₃(NH)₃(NH₂)₃, CH₄, H₂, NH₃, CH₃, NH₂, H.

The thermodynamic data for all the considered species are reported as Supporting Information in Table S1. The reliability of the adopted thermodynamic data can be checked through comparison with the available few experimental data. It is thus interesting to observe that the calculated Ga(CH₃)₃ standard formation enthalpy, -7.4 kcal/mol, is in good agreement with the value recommended by the NIST thermochemical Web site: -8.6 ± 2.4 kcal/mol, as well as the enthalpies of formation of NH₃ (-10.55 kcal/mol calculated versus -10.98 ± 0.084 kcal/mol) and CH₄ (-17.3 kcal/mol calculated versus -17.8 ± 0.1 kcal/mol). Equilibrium calculations were performed by minimizing the Gibbs free energy of the system assuming a pressure of 0.2 bar and initial mole fractions of 0.25 for NH₃, 0.7495 for H₂ and 5.0 × 10⁻⁴ for Ga(CH₃)₃. These conditions correspond to those often adopted to deposit high quality GaN films.^{1,6-8} Simulations were performed in the 700-1500 K temperature range. The results are reported in Figure 1a, for GaXYZ species (with X,Y, Z either CH₃, NH₂, or H), CH₄, NH₃, and H₂, in Figure 1b for species containing 2 or 3 Ga atoms, and in Figure 1c for the decomposition fragments of the growth precursors.

As it can be noted, Ga(CH₃)₃ is present in such a low concentration that it does not even fit in Figure 1a. This is because it is highly unstable, even at room temperature, with respect to the chemical species that can be formed through substitution of methyl with amino groups and atomic H. This is clearly related to the quite high N/C and H/C ratio of the simulated gas phase composition. This is consistent with the results of the thermodynamic analysis performed by Timoshkin et al.^{30,31} using thermodynamic data computed from DFT calculations. The decomposition and conversion of TMGa during GaN growth is thus controlled only by kinetic limitations. In an infinite time, Ga-CH₃ groups would systematically be substituted by the more stable Ga-NH₂ groups. This behavior is consistent with experimental mass spectrometry investigations,^{14,15} which highlight how with increasing temperature it is possible to observe the formation of a dimer of the Ga(CH₃)₂NH₂ species. The formation of the TMGa:NH₃ adduct was not considered in the present analysis, as it is known that it is fully dissociated at temperatures higher

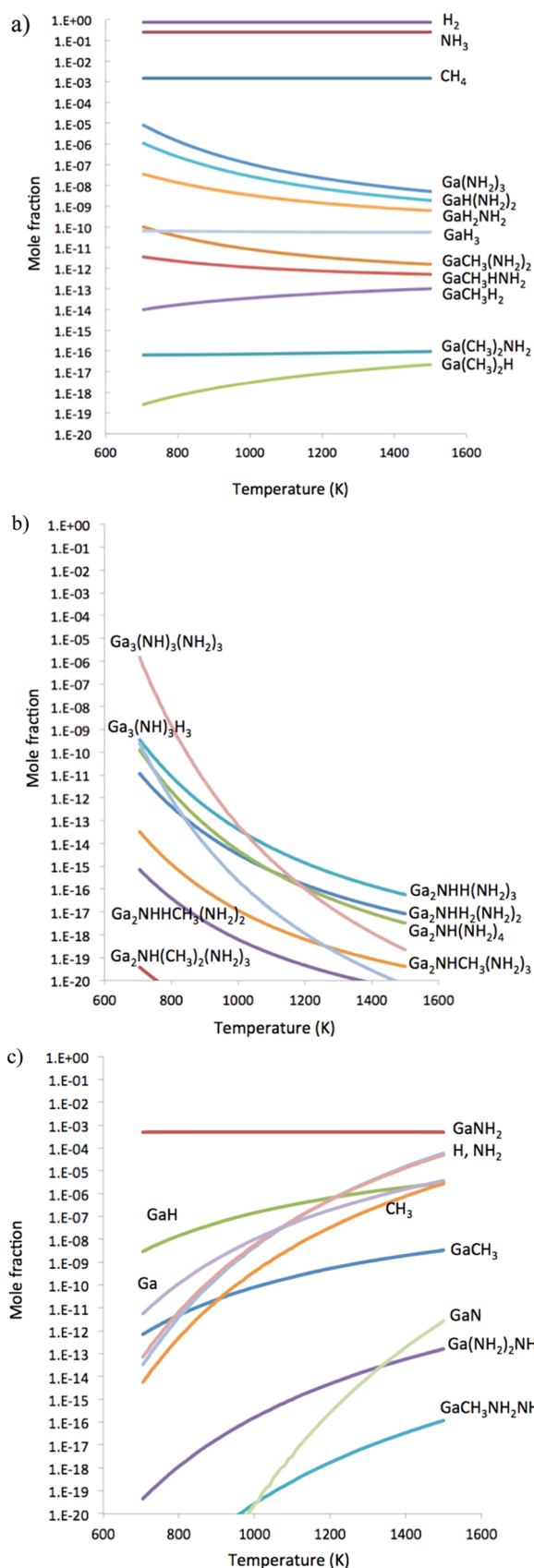


Figure 1. Calculated equilibrium distribution of several gas phase species expected to play a role during the MOVPE of GaN. Calculations performed at constant T , at a pressure of 0.2 bar, and for the following global gas phase composition: 0.25 NH_3 , 0.75 H_2 , and 5.0×10^{-4} $\text{Ga}(\text{CH}_3)_3$.

than 500 K, which is well below the temperature range here investigated.

The equilibrium mole fractions of the considered gas phase species containing 2 or 3 Ga atoms are compared in Figure 1b, while their molecular structures are shown in Figure 2a,c.

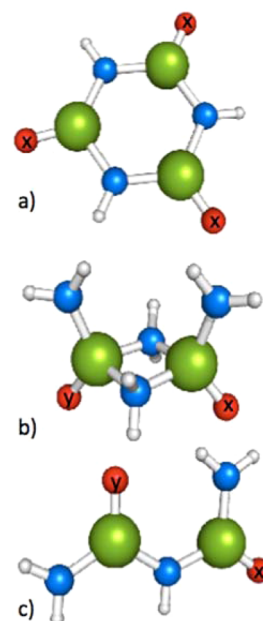


Figure 2. Structures of gas phase species containing three (a: $\text{Ga}_3(\text{NH})_3\text{X}_3$) and two (b: $\text{Ga}_2(\text{NH}_2)_4\text{XY}$; c: $\text{Ga}_2\text{NH}(\text{NH}_2)_2\text{XY}$) Ga atoms that were considered among the possible candidates to be included in the thermodynamic analysis. X and Y may be either CH_3 , NH_2 , or H. Structure b was found to be unstable with respect to structure c at the temperatures here considered, and was therefore not included in the thermodynamic calculations.

The structure reported in Figure 2b is a Lewis acid–base complex resulting by the addition of 2 $\text{TMGa}:\text{NH}_3$ adducts. Compared to the $\text{Ga}(\text{CH}_3)_3:\text{NH}_3$ adduct, this structure is stabilized from the energetic point of view through the formation of two additional acid base bonds. This adduct was initially considered in the calculations as there are experimental evidence that dimers with this composition are formed at low temperatures in $\text{TMGa}–\text{NH}_3$ systems.^{25–27} However, our simulations evidenced that, as the temperature is increased, these species easily eliminate ammonia to form chemical species with the structure shown in Figure 2c, whose formation was as well experimentally observed, and that was therefore considered in the simulations. Also in this case it was found that methylated Ga species are highly unstable. Indeed the $\text{Ga}_2\text{NH}(\text{CH}_3)_4$ equilibrium mole fraction is so small that it can not even be reported in Figure 1b.

The two considered Ga3 species, whose structures are shown in Figure 2a, are $\text{Ga}_3(\text{NH})_3\text{H}_3$ and $\text{Ga}_3(\text{NH})_3(\text{NH}_2)_3$. Similar structures have already been proposed as possible GaN nuclei in previous theoretical studies.^{17,21} The two species have a planar structure characterized by a 6 atoms ring containing 3 Ga and 3 N atoms. As it can be observed, it is predicted that these species become more stable than Ga2 species as the temperature decreases below 1100 K, suggesting that in these conditions Ga2 species may be rapidly converted to larger species and that Ga3 species with structures similar to that

Table 1. Gas Phase Kinetic Mechanism for GaN MOVPE Deposition from TMGa and NH₃^a

	reaction	A	α	E _a		reaction	A	α	E _a
Decomposition of GaXYZ Species (X,Y,Z = CH ₃ , NH ₂ , or H)					Ammino/Methyl Substitution in GaXYZ Species				
G1	Ga(CH ₃) ₃ → GaCH ₃ + 2CH ₃	9.0 × 10 ¹⁶	0.04	79.07	G33	Ga(CH ₃) ₃ + NH ₂ → Ga (CH ₃) ₂ NH ₂ + CH ₃	4.9 × 10 ⁶	2.47	-1.45
G2	Ga(CH ₃) ₂ NH ₂ → GaNH ₂ + 2CH ₃	1.2 × 10 ²⁷	-3.20	81.38	G34	Ga(CH ₃) ₂ NH ₂ + NH ₂ → GaCH ₃ (NH ₂) ₂ + CH ₃	3.7 × 10 ³	2.93	-2.63
G3	GaCH ₃ (NH ₂) ₂ → GaNH ₂ + CH ₃ + NH ₂	1.9 × 10 ¹⁸	-0.59	81.66	G35	GaCH ₃ (NH ₂) ₂ + NH ₂ → Ga (NH ₂) ₃ + CH ₃	2.1 × 10 ³	2.87	-2.85
G4	Ga(NH ₂) ₃ → GaNH ₂ + 2NH ₂	1.9 × 10 ¹⁴	0.26	92.66	G36	GaCH ₃ HNNH ₂ + NH ₂ → GaH (NH ₂) ₂ + CH ₃	6.5 × 10 ³	2.92	-2.34
G5	GaH(NH ₂) ₂ → GaNH ₂ + NH ₂ + H	3.2 × 10 ¹⁶	-0.40	87.60	G37	GaCH ₃ + NH ₂ → GaNH ₂ + CH ₃ NH ₂ and H Abstraction Reactions	2.0 × 10 ⁶	2.46	-1.43
G6	GaCH ₃ HNNH ₂ → GaNH ₂ + CH ₃ + H	4.0 × 10 ²⁴	-2.60	79.94	G38	Ga(CH ₃) ₂ NH ₂ + H → GaCH ₃ + CH ₃ + NH ₃	1.4 × 10 ⁸	1.61	6.41
CH ₃ ,NH ₂ ,H Radical Reactions					G39	GaCH ₃ (NH ₂) ₂ + H → GaNH ₂ + CH ₃ + NH ₃	4.6 × 10 ⁷	1.69	2.90
G7 ^{54,55}	CH ₃ + NH ₃ → NH ₂ + CH ₄	2.5 × 10 ³	2.86	14.60	G40	Ga(NH ₂) ₃ + H → GaNH ₂ + NH ₂ + NH ₃	6.3 × 10 ⁷	1.69	4.42
G8 ^{54,55}	NH ₂ + CH ₄ → CH ₃ + NH ₃	3.1 × 10 ¹	3.59	9.02	G41	GaH(NH ₂) ₂ + H → GaNH ₂ + NH ₂ + H ₂	1.4 × 10 ⁹	1.60	2.51
G9 ⁵⁶	CH ₄ + H → CH ₃ + H ₂	1.3 × 10 ⁴	3.00	8.03	G42	GaCH ₃ HNNH ₂ + H → GaNH ₂ + CH ₃ + H ₂	1.6 × 10 ⁻⁴	5.80	0.03
G10 ⁵⁶	CH ₃ + H ₂ → CH ₄ + H	6.9 × 10 ³	2.74	9.42	Condensation Reactions (and Reverse Processes)				
G11 ⁵⁷	H + NH ₃ → NH ₂ + H ₂	5.8 × 10 ⁴	2.76	10.27	G43	2GaH(NH ₂) ₂ → Ga ₂ NHH ₂ (NH ₂) ₂ + NH ₃	4.7 × 10 ⁻²	2.87	-16.53
G12 ⁵⁷	NH ₂ + H ₂ → NH ₃ + H	1.6 × 10 ³	2.83	7.23	G44	Ga ₂ NHH ₂ (NH ₂) ₂ + NH ₃ → 2GaH(NH ₂) ₂	6.0 × 10 ⁻²	3.11	-12.55
G13 ^{58a}	C ₂ H ₆ → 2CH ₃ (0.2 bar)	2.1 × 10 ⁴⁸	-9.72	101.87	G45	2GaCH ₃ (NH ₂) ₂ → Ga ₂ NH (CH ₃) ₂ (NH ₂) ₂ + NH ₃	7.8 × 10 ⁻³	2.92	-16.36
G14 ^{58a}	2CH ₃ → C ₂ H ₆	8.1 × 10 ³⁵	-7.14	7.62	G46	Ga ₂ NH(CH ₃) ₂ (NH ₂) ₂ + NH ₃ → 2GaCH ₃ (NH ₂) ₂	3.1 × 10 ⁻³	3.73	-12.10
G15 ^{58a}	CH ₄ → CH ₃ + H	5.01 × 10 ³⁶	-6.77	110.83	G47	2Ga(NH ₂) ₃ → Ga ₂ NH(NH ₂) ₄ + NH ₃	2.6 × 10 ⁻³	2.81	-14.62
G16 ^{58a}	CH ₃ + H → CH ₄	4.37 × 10 ³⁴	-6.77	5.38	G48	Ga ₂ NH(NH ₂) ₄ + NH ₃ → 2Ga (NH ₂) ₃	2.3 × 10 ⁻²	3.16	-8.21
Hydride Decomposition Reactions					G49	GaCH ₃ (NH ₂) ₂ + GaH(NH ₂) ₂ → Ga ₂ NHHCH ₃ (NH ₂) ₂ + NH ₃	7.6 × 10 ⁻⁴	3.40	-16.50
G17	GaCH ₃ HNNH ₂ → GaNH ₂ + CH ₄	2.2 × 10 ¹¹	0.79	70.63	G50	Ga ₂ NHHCH ₃ (NH ₂) ₂ + NH ₃ → GaCH ₃ (NH ₂) ₂ + GaH(NH ₂) ₂	2.19 × 10 ⁻³	3.63	-12.32
G18	GaCH ₃ HNNH ₂ → GaCH ₃ + NH ₃	1.1 × 10 ¹³	0.21	63.10	G51	GaCH ₃ (NH ₂) ₂ + Ga(NH ₂) ₃ → Ga ₂ NHCH ₃ (NH ₂) ₃ + NH ₃	8.3 × 10 ⁻³	2.87	-14.01
G19	GaH(NH ₂) ₂ → GaNH ₂ + NH ₃	1.2 × 10 ¹³	0.20	60.82	G52	Ga ₂ NHCH ₃ (NH ₂) ₃ + NH ₃ → GaCH ₃ (NH ₂) ₂ + Ga(NH ₂) ₃	8.5 × 10 ⁻³	3.12	-8.95
GaXYZ + Ammonia (X,Y,Z = CH ₃ , NH ₂ , or H) Reactions					G53	GaH(NH ₂) ₂ + Ga(NH ₂) ₃ → Ga ₂ NHH(NH ₂) ₃ + NH ₃	1.9 × 10 ⁻²	2.84	-14.20
G20	Ga(CH ₃) ₃ + NH ₃ → Ga (CH ₃) ₂ NH ₂ + CH ₄	2.57 × 10 ⁰	3.39	14.59	G54	Ga ₂ NHH(NH ₂) ₃ + NH ₃ → GaH (NH ₂) ₂ + Ga(NH ₂) ₃	1.5 × 10 ⁻²	3.08	-9.22
G21	Ga(CH ₃) ₂ NH ₂ + NH ₃ → GaCH ₃ (NH ₂) ₂ + CH ₄	2.9 × 10 ⁻¹	3.84	20.99	H/NH ₂ Substitution in GaXYZ Species				
G22	GaCH ₃ (NH ₂) ₂ + NH ₃ → Ga (NH ₂) ₃ + CH ₄	1.2 × 10 ⁰	3.49	24.93	G29	Ga(NH ₂) ₃ + H → GaH(NH ₂) ₂ + NH ₂	4.4 × 10 ¹²	0.15	7.10
G23	GaCH ₃ + NH ₃ → GaNH ₂ + CH ₄	8.3 × 10 ¹	3.25	18.09	G30	GaH(NH ₂) ₂ + NH ₂ → Ga(NH ₂) ₃ + H	7.1 × 10 ⁴	2.33	-2.00
G24	GaCH ₃ HNNH ₂ + NH ₃ → GAH (NH ₂) ₂ + CH ₄	2.0 × 10 ⁰	3.48	21.7	G31	GaCH ₃ (NH ₂) ₂ + H → GaH (NH ₂) ₂ + CH ₃	4.7 × 10 ¹¹	0.78	0.71
G25	GaH(NH ₂) ₂ + NH ₃ → Ga(NH ₂) ₃ + H ₂	5.2 × 10 ¹	3.16	23.06	G32	Ga(CH ₃) ₂ NH ₂ + H → GaCH ₃ HNNH ₂ + CH ₃	5.0 × 10 ¹¹	0.82	0.35
G26	Ga(NH ₂) ₃ + H ₂ → GaH(NH ₂) ₂ + NH ₃	3.6 × 10 ⁷	1.28	29.49					
G27	GaCH ₃ HNNH ₂ + NH ₃ → GaCH ₃ (NH ₂) ₂ + H ₂	2.9 × 10 ⁰	3.48	19.25					
G28	GaCH ₃ (NH ₂) ₂ + H ₂ → GaCH ₃ HNNH ₂ + NH ₃	8.5 × 10 ⁵	1.83	28.36					

^aCalculated using Troe parameters and interpolated at 0.2 bar.⁵⁸

^aUnimolecular rate constants in s⁻¹ and bimolecular rate constants in cm³/mol/s. Activation energies in kcal/mol. Reactions G13–G16 are pressure dependent, and the rate constants are computed at 0.2 bar. All backward rate constants, where relevant, are explicitly reported.

shown in Figure 2a may indeed be the initial nuclei whose successive growth may lead to the formation of GaN powders.

The equilibrium mole fractions of the molecular and radical fragments that may be formed as a result of the decomposition of the molecules reported in Figure 1a are shown in Figure 1c. As it can be observed, the most stable species is GaNH₂, followed by NH₂, H, Ga, and GaH. The GaNH₂ equilibrium mole fraction is almost independent of temperature, as it is the most abundant Ga species, so that its formation is controlled by the relative amount of Ga atoms assumed to be present in the gas phase. The biatomic species GaN is predicted to be much

less stable in the full temperature range. This is a quite interesting result with important implications, as GaNH₂, Ga, and GaN have been postulated by different authors to be possible precursors to the film growth.^{3,4,18,24} The present thermodynamic analysis suggests that, if the reactivity is sufficiently fast to let the system approach equilibrium, then GaNH₂ should be the most likely gas phase precursor to GaN growth. However, the calculated equilibrium mole fraction of GaNH₂ is so high that it seems strange that it was not detected in previous mass spectroscopic investigation. While the limited temperature range investigated by Bergmann et al. (up to 1000

K) may be an explanation of the reason why GaNH₂ was not detected,¹⁴ this is not the case for the study of Schafer et al.,¹⁵ who investigated a temperature range extending up to 1400 K. It is, however, noteworthy to point out that Schafer et al. found that above 900 K the most abundant gas phase species that is detected is atomic Ga. As they performed their experiments using a ionization electron energy of 30 eV, it is possible that the Ga signal may have been originated by the dissociative ionization of GaNH₂. Indeed, it is known that methyl groups are labile upon ionization in TMGa, and the same may be possible for NH₂.⁵² Although this explanation would reconcile experiment and theory, we feel that additional experiments performed with the aim of detecting the GaNH₂ signal would be crucial in determining which is the GaN growth precursor. It is finally interesting to observe that GaNH₂ was indeed experimentally found to be the main product that is formed when Ga atoms and ammonia dispersed in an Ar matrix are photoactivated.⁵³

3.2. Gas Phase Kinetic Mechanism. The gas phase kinetic mechanism here proposed is summarized in Table 1, together with rate constants interpolated between 300 and 1500 K. The following criteria were followed to select the present list of reactions. The thermodynamic analysis indicated that, in the conditions at which GaN is deposited, TMGa is unstable, both because its unimolecular fragmentation into GaCH₃ and methyl proceeds fast and because the substitution of its methyl groups with amino groups and H atoms is thermodynamically favored and kinetically fast. In order to properly describe the reactivity of TMGa and to limit the total number of gas phase species, it was decided to include in the calculations those species that can be generated from amino and H substitution of CH₃ groups: Ga(CH₃)₃, Ga(CH₃)₂NH₂, GaCH₃(NH₂)₂, Ga(NH₂)₃, GaH(NH₂)₂, and GaCH₃HNH₂. The formation of Ga species with two or three H atoms was thus discarded, as they are less stable than Ga(NH₂)₃ and GaH(NH₂)₂ and since their formation would require the full conversion of TMGa, in which case it is expected that amino substituted species would be the most abundant. Also, it was assumed that all these species can undergo homolytic decomposition. As it is known that after TMGa loses the first methyl group, it rapidly decomposes further to also lose the second and yield GaCH₃, it was decided to lump together the two decomposition reactions. Similarly, it was assumed that also other reactions leading to the formation of GaXY species (X,Y = CH₃, NH₂ or H), such as reactions G38–G42, would be followed by a successive cleavage of the weakest GaXY bond. Also, in this case, the two reactions were lumped. The considered decomposition reactions, G1–G6, are listed in Table 1 together with the calculated high pressure rate constants. Rate constants for decomposition reactions G1–G6 were calculated using variational transition state theory, as they proceed without passing from a saddle point. The energy changes calculated for reactions G1–G6 at different levels of theory are summarized in Table 2. Reaction rates were calculated for the scission of the most labile bond. The progress of reactions G1–G6 leads to the formation of GaNH₂, GaCH₃, CH₃, NH₂, and H. In order to describe the reactivity of CH₃, NH₂, and H reactions G7–G16 were included in the kinetic mechanism. The rate constants of these reactions are well-known and were therefore taken from the literature. Hydride species GaH(NH₂)₂ and GaCH₃HNH₂ can also decompose at rates comparable to G5 and G6 eliminating ammonia and methane. To describe these processes, which

Table 2. Energy changes for the reactions of decomposition of Ga(CH₃)₃, Ga(CH₃)₂NH₂, GaCH₃(NH₂)₂, Ga(NH₂)₃, GaH(NH₂)₂, and GaCH₃HNH₂ calculated at different levels of theory. All energies include Zero Point Energy corrections

reaction	energy change (kcal/mol)	
	M062X/6-311+G(d,p)	ROCBS-QB3
Ga(CH ₃) ₃ → GaCH ₃ + 2CH ₃	73.5	77.4
Ga(CH ₃) ₂ NH ₂ → GaNH ₂ + 2CH ₃	74.5	78.5
GaCH ₃ (NH ₂) ₂ → GaNH ₂ + CH ₃ + NH ₂	76.8	81.5
Ga(NH ₂) ₃ → GaNH ₂ + 2NH ₂	90.9	94.2
GaH(NH ₂) ₂ → GaNH ₂ + NH ₂ + H	79.6	85.6
GaCH ₃ HNH ₂ → GaNH ₂ + CH ₃ + H	74.2	78.0

occurs through tight transition states, reactions G17–G19 were also included in the kinetic mechanism.

Two reaction classes were introduced in order to describe the inter conversion kinetics among the considered GaXYZ species (where X, Y, Z can be CH₃, NH₂, or H). In the first reaction class, GaXYZ reacts with ammonia to substitute methyl or H with an amino group (reactions G20–G28). The transition state structure of reaction G20 is reported in Figure 3a. As already pointed out in earlier studies,²¹ these reactions

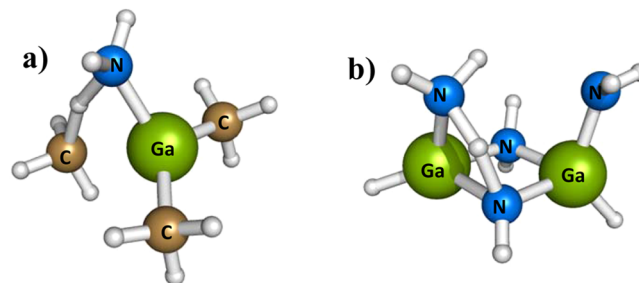


Figure 3. Structures of transition states of reactions (a) Ga(CH₃)₃ + NH₃ → Ga(CH₃)₂NH₂ + CH₄ and (b) 2GaH(NH₂)₂ → Ga₂NHH₂(NH₂)₂ + NH₃.

take place in two steps. The first is the formation of Lewis acid–base adducts, such as Ga(CH₃)₃:NH₃ for reaction G20, which is a precursor state whose formation does not require overcoming any energy barrier. The second step is the elimination of a methane (or H₂) molecule, which takes place through a tight transition state. As explained in the previous section the ammonia adduct is very unstable and it is rapidly decomposed above 500 K. Thus, the rate of these reactions is controlled by the tight transition state and can be calculated using conventional transition state theory.

In the second reaction class GaXYZ adds NH₂ and releases either H or CH₃ through reactions G29–G37, which can be considered as a set of propagation reactions of a radical chain mechanism started by reactions G1–G6. This set of reactions was proposed by our group about a decade ago to be the main mechanism of insertion of amino groups in Ga compounds. The rate constants of these reactions were estimated in our previous study using the kinetic theory of gases, as they proceed without overcoming any energy barrier. Indeed, similarly to what is found for the reactions between ammonia and GaXYZ, these processes proceed through the formation of an intermediate adduct of NH₂ with GaXYZ that successively

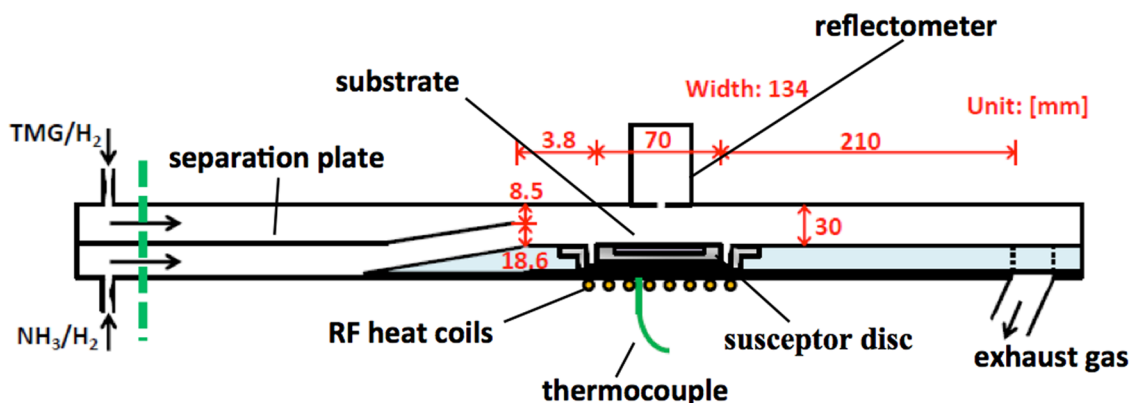


Figure 4. Geometry of the AIX200/4 reactor used to model the gas phase kinetics active during GaN MOVPE.

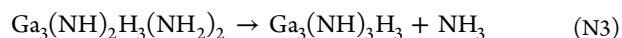
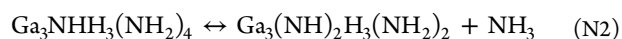
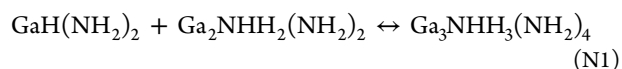
decomposes, releasing H or CH₃. The reactions are globally exothermic, and no energy barriers are present both on the entrance and on the exit channels of the PES. Given the exothermicity of these reactions, their rate can be reasonably assumed to be equal to that of the entrance channel. High pressure rate constants were then determined using variational transition state theory and assumed to be equal to the rate of formation of the complex between NH₂ and GaXYZ. The variational rate constants differ by about a factor of 4 from the collisional estimates, which can be considered reasonable given the uncertainties of both approaches.

Since in the conditions in which GaN is deposited atomic H can be present in significant concentrations, it is possible that it may react with GaXYZ species to abstract either NH₂ or H. These reactions, which proceed through a tight transition state, have small activation energies and are thus expected to proceed fast. Reactions G38–G42 were introduced in the kinetic mechanism to account for this reaction route. Abstraction of methyl groups was found to proceed at a rate significantly slower than that for abstraction of NH₂ or H, because of larger energy barriers.

Reactions G1–G42 describe several possible reaction routes, in some cases competitive with one another, that lead to the inter conversion between the GaXYZ species and to the formation of their decomposition products. Following the development of this part of the kinetic mechanism, the possible reactivity among this species was investigated in order to determine which are the fastest pathways that may lead to the formation of the GaN nuclei that precedes the formation of powders. As explained in the previous section, it is reasonable to assume that the first stable nuclei will contain at least three Ga atoms participating to six-membered cyclic species. It is thus clear for kinetic reasons that, in order to form the first GaN nuclei, it will be necessary to form an intermediate species containing two Ga atoms. In our previous studies^{17,21} we hypothesized that such species could be formed through a radical chain mechanism that implied the formation of a radical GaXYZ• species as an intermediate species. In the present study we propose a new set of reactions that proceed much faster than the mechanism we previously proposed as it involves as reactants two GaXYZ species, with both reactants containing at least one amino group, and not radicals. These reactions proceed through the formation of a Lewis acid–base adduct (see Figure 2b), which successively decomposes fast through a tight transition state (Figure 3b) having an energy barrier that is smaller than that of the reactants. At GaN deposition temperature, the adduct is unstable with respect to

the reactants, and the reaction rate is controlled by the tight transition state. The condensation reactions considered to be relevant for the formation of Ga species with 2 Ga atoms are reactions G43–G54 reported in Table 1.

Finally, some preliminary studies were performed in order to investigate the reaction mechanism that leads to the formation of the first particle aggregates. It is reasonable to expect that the condensation products formed through reactions G43–G54 may successively react with a GaXYZ species through a similar mechanism to form a nuclei having a structure equivalent to that reported in Figure 2a. A preliminary analysis indicated that a fast reaction pathway is possible if the product of the condensation reacts with a GaXYZ species containing at least two amino groups. The mechanism leading to the formation of the nuclei may then be described by the following set of reactions, here referred to make a practical example to the GaH(NH₂)₂ and Ga₂NHH₂(NH₂)₂ reactants:



Steps N1 and N2 are quite similar to the reaction mechanism that was found for condensation reactions: formation of a Lewis acid–base adduct followed by its decomposition through the loss of an ammonia molecule. As found for condensation reactions, in this case the formation of the adduct is also barrierless, while for its decomposition several transition states are possible, all with energy barriers lying well below the energy of the reactants. Actually, a preliminary analysis of reactions N1 and N2 suggests that the rate limiting step for this reaction sequence is the formation of the adduct through N1, since we were able to find at least one transition state with a quite low energy barrier, due to stabilization through intramolecular donor–acceptor interactions. This preliminary analysis also showed that reaction N3 is likely to proceed fast, thus suggesting that the rate-determining step of this reaction pathway may be the collision between the condensation product and GaX(NH₂)₂, rather than the subsequent reaction steps. Since at present it is difficult to determine a rate constant for this process, as the vibrational analysis of the PES of reaction N1 showed that it is highly anharmonic and that multiple pathways leading to the same products are possible, we conclude this kinetic analysis suggesting that the rate of formation of the first nuclei will be proportional to the

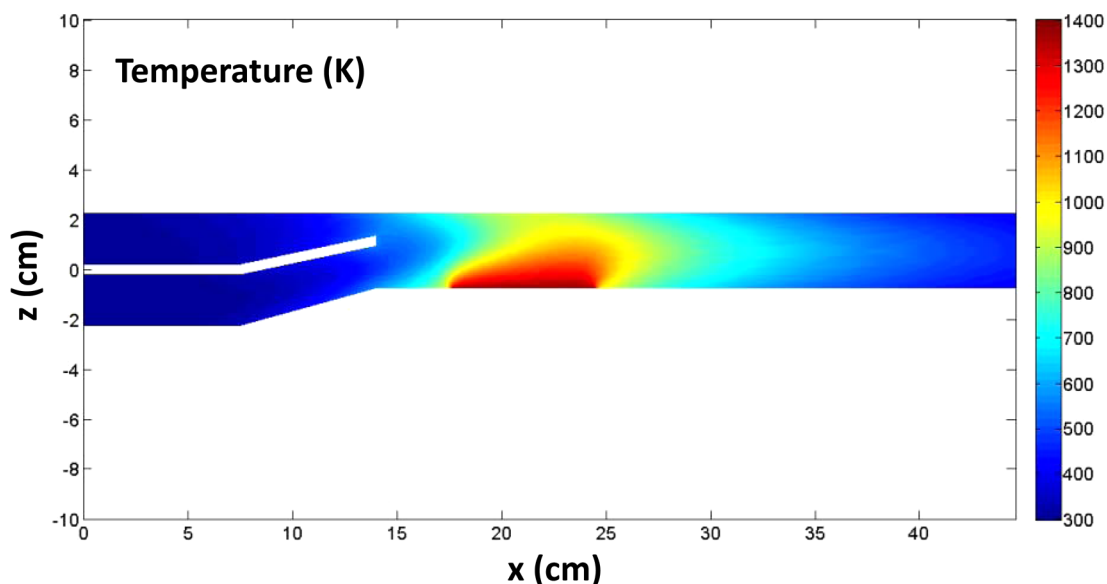


Figure 5. Temperature field (K) of the AIX200/4 reactor computed in the operative conditions of Table 3 for a substrate temperature of 1400 K.

concentration of the $\text{Ga}_2\text{NH}(\text{NH}_2)_2\text{XY}$ condensation products and of the $\text{GaX}(\text{NH}_2)_2$ species (with $\text{X} = \text{CH}_3, \text{H}, \text{or } \text{NH}_2$), with a rate constant that is probably close to the collisional limit. While it is quite difficult to find a direct experimental confirmation of the proposed mechanism of nucleation of GaN powders, an indirect confirmation that our proposal may be pointing in the right direction comes from the solution chemistry study performed by Jegier et al.,⁵⁹ who showed that poly(imidogallane) $[\text{HGaNH}]_n$ is an intermediate in the conversion of cyclotrigallazane $[\text{H}_2\text{GaNH}_2]_3$ to nanocrystalline GaN poly(imidogallane). Indeed, both the $\text{Ga}_2\text{NHH}_2(\text{NH}_2)_2$ (and similar) chemical species that we propose to be formed as an intermediate before the nucleation of the first powder nuclei, as well the structure we propose for the first nuclei, $\text{Ga}_3(\text{NH})_2\text{H}_3(\text{NH}_2)_2$, possess the imido bonds of $[\text{HGaNH}]_n$, thus indicating that both the mechanism here proposed and the one found to be active for the conversion of cyclotrigallazane to GaN nanocrystals may involve the formation of similar intermediates.

3.3. Analysis of the Gas Phase Reactivity. The gas phase reactivity was investigated embedding the kinetic mechanism described in section 3.2 into a 2D model of the single wafer horizontal reactor AIX200/4, which has been often used to deposit GaN nitride thin films.^{5–7} A sketch of the reactor configuration is shown in Figure 4, while the simulated temperature profile is reported in Figure 5. Simulations were performed assuming that GaNH_2 decomposes upon collision with the surface to give GaN and H_2 . Transport parameters for all the considered gas phase species were computed from Lennard-Jones parameters using Chapman–Enskog theory, as described by Reid et al.⁶⁰

The Operative Conditions Used in the Simulations Are Those Usually Adopted to Deposit High Quality GaN Films and Are Summarized in Table 3.

The calculated gas phase concentrations of the GaXYZ species are reported in Figure 6.

The mole fraction distributions of the GaXYZ species shown in Figure 6 show how the methyl groups of $\text{Ga}(\text{CH}_3)_3$ are gradually substituted with amino group as soon as the reactant enters the reactor heated zone. This is determined both by

Table 3. Operative Conditions Used to Simulate GaN Deposition in the AIX200/4 Reactor

variable	operative conditions
substrate temperature	1400 K
flow rate upper channel	3.5 slm
flow rate lower channel	6.5 slm
total pressure	200 mbar
$\text{Ga}(\text{CH}_3)_3$ pressure	6.9×10^{-2} mbar
NH_3 pressure	50 mbar

direct reaction of ammonia with GaXYZ, followed by elimination of methane and molecular hydrogen (reactions G20–G28), and by the radical propagation reactions G29–G37. This reaction pathway is clearly favored by the fact that GaN is usually deposited with a large excess of ammonia with respect to Ga. It is, however, interesting to observe that $\text{Ga}(\text{NH}_2)_3$ is not the most abundant species, though it is the one that is predicted to be the most stable through equilibrium calculations, thus indicating that the system reactivity is controlled by kinetics. The important role of this reaction set had already been previously inferred by Ikeda et al.,²³ as well as by our research group.^{17,21} It is, however, interesting to observe that a considerable amount of hydride species is predicted to be formed above the susceptor, in a concentration comparable to those of the most stable GaXYZ species. Once formed, hydrides can decompose fast to GaNH_2 through reactions G17–G19. These reactions take place together with decomposition reactions of GaXYZ as the gas approaches the heated susceptor. The calculated mole fraction of the most abundant fragments of GaXYZ are compared in Figure 7.

The data reported in Figure 7 show how, as the temperature increases, GaXYZ species become unstable and decompose to GaNH_2 , GaCH_3 , CH_3 , NH_2 , and H. In particular, in agreement with the equilibrium calculations, we found that GaNH_2 is the most abundant species that is formed above the susceptor, which confirms its identification as the main GaN growth precursor. GaCH_3 is present in concentrations that are about 2 orders of magnitude smaller than those of GaNH_2 .

One of the several reaction routes that can lead to the formation of GaNH_2 is the following:

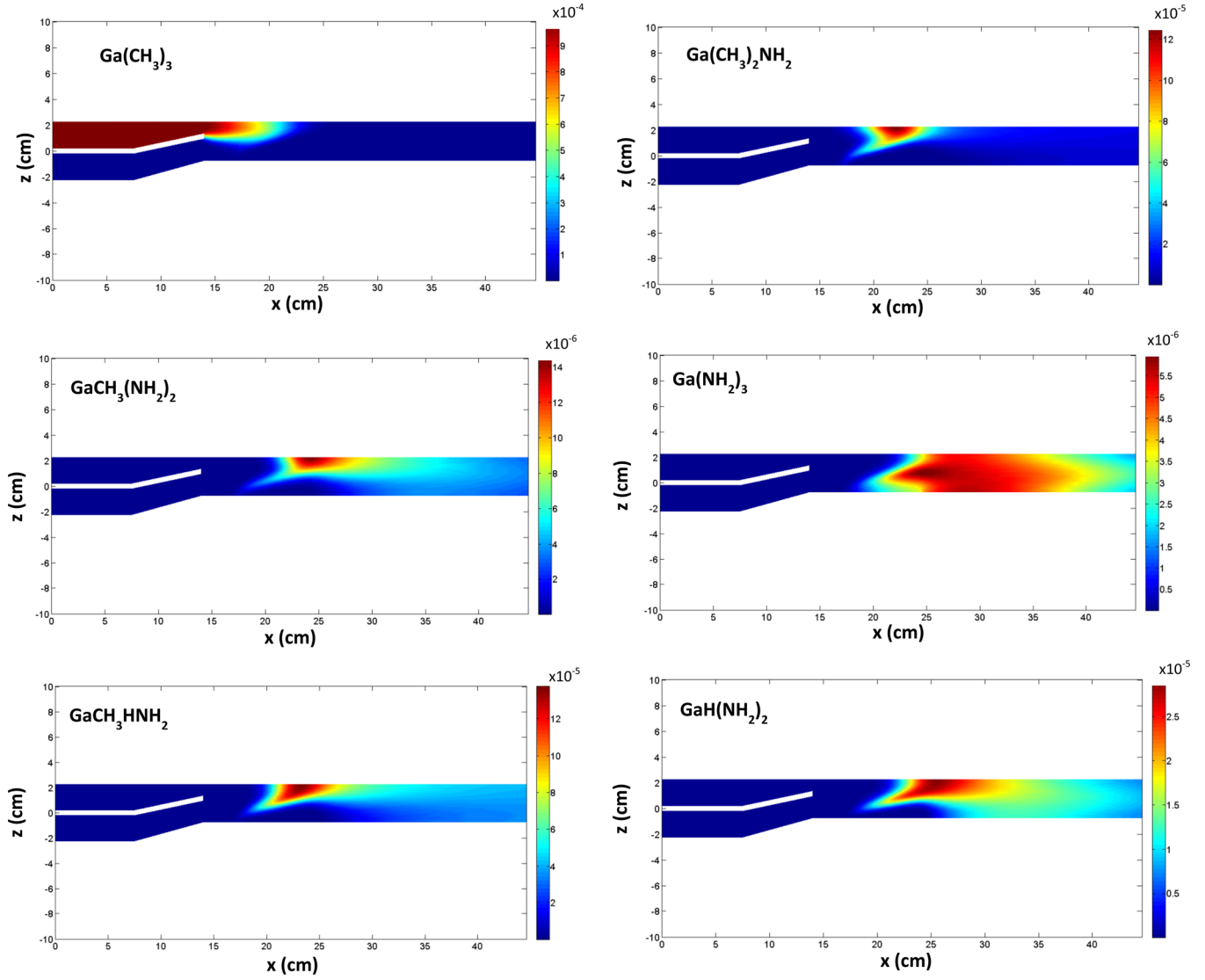
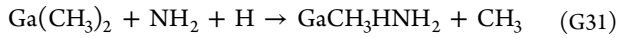
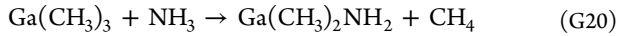


Figure 6. Distribution of the mole fractions of GaXYZ species in the AIX200/4 reactor computed in the operative conditions of Table 3 for a substrate temperature of 1400 K.



Although this cascade of reactions proceeds fast as the temperature increases, it is not the only pathway that leads to the formation of GaNH₂. A summary of the main reaction pathways that are active during GaN deposition in the investigated set up is reported in Figure 8.

As it is known, a powder nucleation mechanism is often active in parallel and in competition with the film growth. As described in the kinetic section, we hypothesize here that the main step that precedes powder nucleation is the formation of chemical species containing 2 Ga atoms through condensation reactions. The calculated mole fractions of the most abundant among these species are reported in Figure 9.

As it can be observed, the two condensation products that are predicted to be formed in the highest concentration are the

same as the chemical species with two Ga atoms that are found to be most stable through thermodynamic simulations. The reason is that both the forward and backward reactions leading to the formation and decomposition of these species are quite fast, so that their relative abundance is controlled by thermodynamics and local composition. This means that high ammonia concentrations hinder the formation of the GaNH-(NH₂)₂XY condensation products, because it accelerates their decomposition reactions. However, high ammonia concentrations also promote the generation of GaX(NH₂)₂, which is the GaNH(NH₂)₂XY reacting partner that leads to the formation of the first stable GaN nuclei, so that it is reasonable to expect that the impact of ammonia concentration on the nucleation of powders may be on the whole limited. The present analysis of the nucleation mechanism is a preliminary work that will be further deepened in our next publication, where simulations will be validated through comparison with experimental data, and a powder formation and growth model will be coupled to the fluid dynamic model.

3.4. Alternative Reaction Pathways. The kinetic mechanism here proposed differs from others that can be

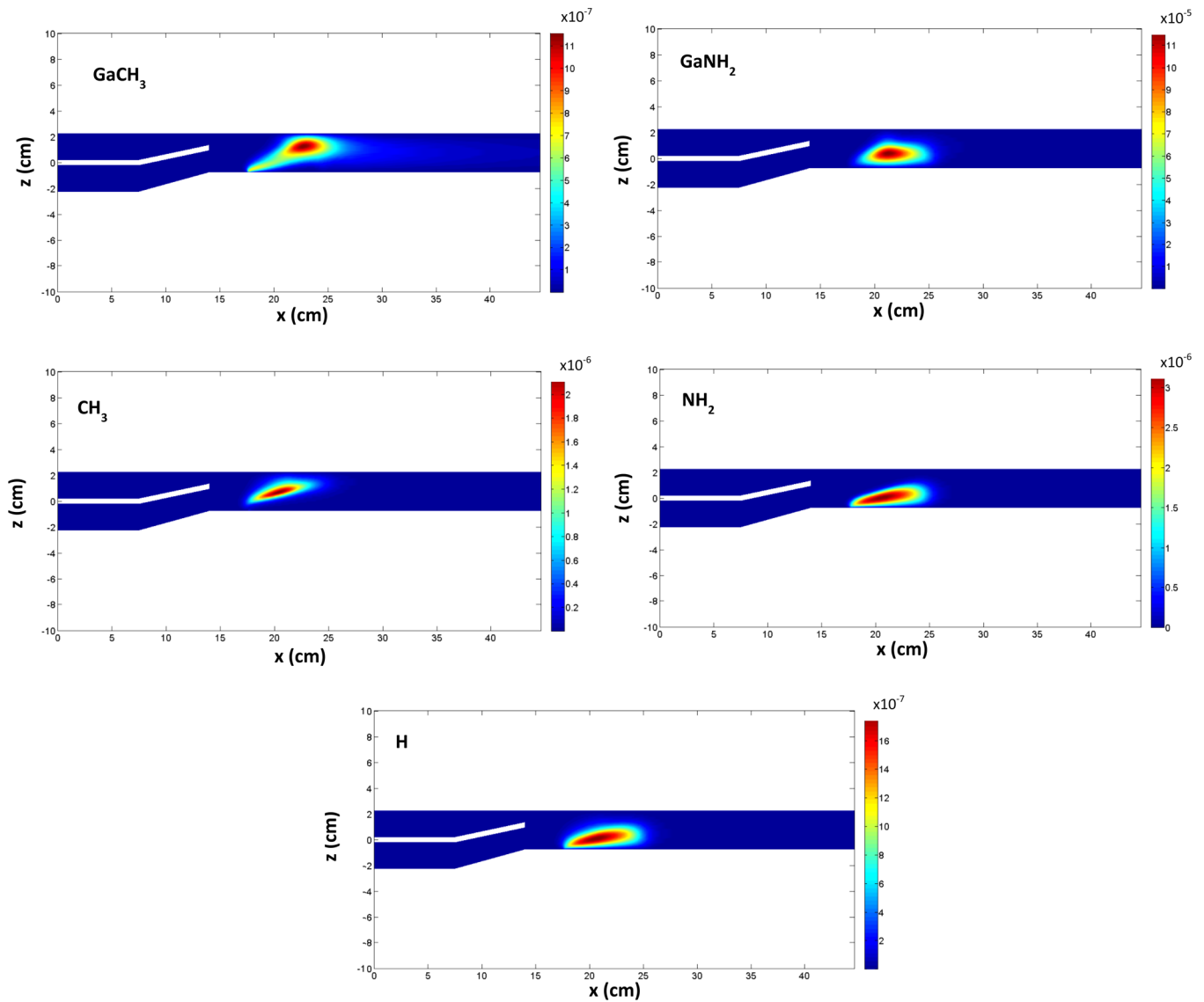


Figure 7. Distribution of the mole fractions of the fragments of GaXYZ species in the AIX200/4 reactor computed in the operative conditions of Table 3 for a substrate temperature of 1400 K.

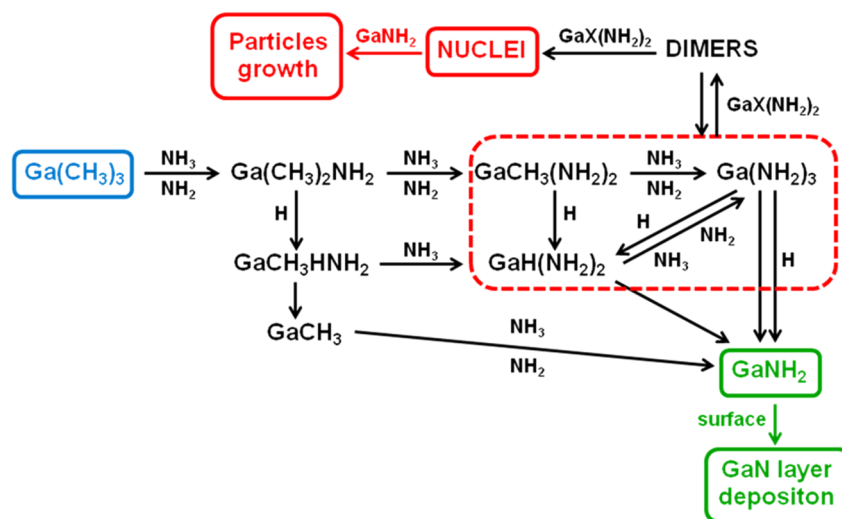


Figure 8. Main reaction pathways that are predicted to be active in the gas phase during GaN MOVPE simulated using the kinetic mechanism reported in Table 1.

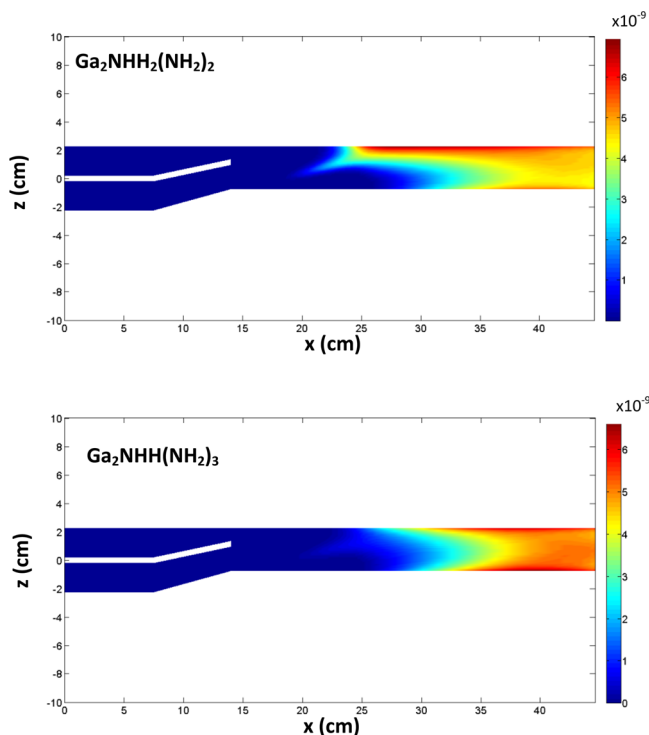
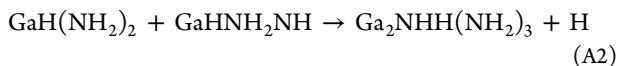


Figure 9. Distribution of the mole fractions of the two most abundant Ga species with two Ga atoms in the AIX200/4 reactor computed in the operative conditions of Table 3 for a substrate temperature of 1400 K.

currently found in the literature and contains a selected set of reactions. In the present section we will discuss why we believe that the present mechanism describes better the GaN kinetics than others mechanisms that have previously been published and we will comment on the reason why several reaction classes were excluded from the present model. On the whole, six alternative or parallel reaction routes were considered and discarded, as proceeding at reaction rates not comparable to those of the reactions listed in Table 1.

(1) The first alternative mechanism that was considered is the radical mechanism that leads to the formation of $\text{GaNH}(\text{NH}_2)_2\text{XY}$ condensation products with the structure shown in Figure 2c that we proposed a few years ago.^{17,21} An example of this mechanism is given by reactions A1 and A2:

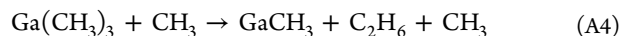
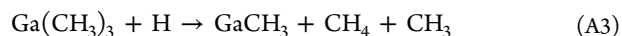


The radical condensation mechanism was compared with the one here proposed (reactions G43–G54) and found to be significantly slower, though its rate constants have quite high values as the system reactivity is almost collisional. The reason is that the concentration of the $\text{GaXYZ}\bullet$ radicals generated in reaction A1 (and others) and consumed in reaction A2 is much smaller than that of the GaXYZ species that, through reactions G43–G54, lead to the formation of the $\text{GaNH}(\text{NH}_2)_2\text{XY}$ species. The ratio between the concentration of GaXYZ and $\text{GaXYZ}\bullet$ was computed inserting some reactions of the radical mechanism in the fluid dynamic model and was found to be comparable to what is predicted through equilibrium simulations (see Figure 1b,c), that is about 10^5 . As the rate constant of reactions G43–G54 are only 2 orders of magnitude

smaller than those of reaction A2 (and others that are similar), it was safely concluded that the contribution of the radical chain mechanism to the formation of $\text{GaNH}(\text{NH}_2)_2\text{XY}$ condensation products is negligible in the investigated conditions. However, it is possible that in conditions different from those here examined, for example, in photoassisted or laser-assisted CVD, the contribution of the radical chain pathway to the system reactivity may become more relevant.

(2) The products of reactions G43–G54 are $\text{GaNH}(\text{NH}_2)_2\text{XY}$ and ammonia. $\text{GaNH}(\text{NH}_2)_2\text{XY}$ species can be produced also through reactive mechanisms whose byproducts are methane or molecular hydrogen. To test the feasibility of these reaction mechanisms, rate constants were computed for some reactions. It was found that these reactions have energy barriers that are more than 20 kcal/mol higher than those of the ammonia pathways with similar pre-exponential factors, so that the rate constants are much smaller. These reaction pathways were therefore neglected as they are not competitive with those already considered.

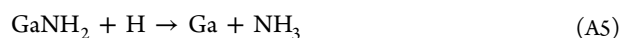
(3) Methyl abstraction reactions from Ga species, which were included in our previous studies assuming that atomic H or methyl may be the extracting radicals,²¹ were not included in the present mechanism, as their rate is much smaller with respect to other competitive reaction pathways that are already included in the mechanism. Two examples of such reactions are



(4) The mechanism proposed by Hirako et al.¹⁸ to model the GaN growth kinetics was considered and discarded, as it is much slower than the mechanism here proposed. The Hirako mechanism postulates, on the basis of DFT calculations and fluid dynamic simulations, that the main GaN growth precursor is the GaN gas phase diatomic molecule, which is also expected to play a quite important role in the powder nucleation mechanism. We examined the Hirako hypothesis quite carefully. First we re-estimated the rate constants calculated by Hirako, which were determined at a level of theory that is lower than the one here considered, as we used a more recent DFT functional that accounts also for dispersion and calculated energies with the hybrid ROCBS-QB3 approach. We found that one of the key reactions of the Hirako mechanism, the decomposition of $\text{Ga}(\text{CH}_3)_2\text{NH}_2$ to give GaCH_3NH and CH_4 , has an energy barrier that is about 30 kcal/mol higher than that predicted by Hirako et al. The energy barrier we computed for this process, 72.8 kcal/mol, is in reasonable agreement with the 76 kcal/mol value calculated by Mondal et al.²² for the same process. Also, Hirako et al. neglected to consider additional reaction pathways for GaCH_3NH , such as the addition of an ammonia molecule to give $\text{GaCH}_3(\text{NH}_2)_2$. We investigated this reaction pathway and found that it is barrierless, thus indicating that, should GaCH_3NH be formed, its main pathway would most likely be that of being converted to $\text{GaCH}_3(\text{NH}_2)_2$. As GaCH_3NH is the only precursor to the GaN diatomic species proposed by Hirako, it was concluded that the mechanism of formation of diatomic GaN proposed by Hirako is not active. This implies that also the powder nucleation mechanism proposed by these authors is not efficient.¹⁸ Finally, we observed that, although alternative mechanism of formation of diatomic GaN may be active in the gas phase, this species is, however, thermodynamically unstable (see Figure 1c), so that, even if it were formed in a non negligible amount in the gas

phase, it is most likely that its fate would be that of being converted back to more stable species, such as GaNH₂. We believe that the reason why several authors were able to model with success the GaN deposition using Hirako model or similar models assuming that the diatomic GaN species is the main precursors to deposition, is that such simulations were usually performed without accounting for backward reactions, as no thermodynamic data were available up to now to calculate backward rate constants. We recommend therefore to perform future simulations of GaN deposition using the thermodynamic data set proposed in the present paper.

(5) As discussed in section 3.1, Shafer et al.¹⁵ proposed on the basis of mass spectroscopic investigation that the main GaN growth precursor may be Ga. To test this proposal, we included in the kinetic mechanism the following reaction of conversion of GaNH₂ to Ga:



This reaction has a small energy barrier of 8 kcal/mol, which means that at the high temperatures that are reached above the growth substrate, where the concentration of GaNH₂ and atomic H is maximum (see Figure 7), atomic Ga may be formed in a significant concentration. However, as shown in Figure 1c, atomic Ga is thermodynamically unstable with respect to GaNH₂, which suggests that, if formed, it should react fast with ammonia to form GaNH₂ through the backward process of reaction A5. Reaction A5 was found to contribute negligibly to the gas phase reactivity and was therefore not included in the gas phase mechanism.

(6) A final important point related to the gas phase reactivity concerns the nature of the chemical species that may be the nucleation precursors. Indeed it has been proposed in the literature that both the compounds reported in Figure 2, (Ga(NH₂)₂X)₂ and Ga₂NH(NH₂)₂XY, in the operative conditions at which GaN is usually deposited may play an important role in the kinetic mechanism of particles formation. Hence, in order to clarify this critical issue, some sensitivity tests were performed assuming that these two species are in thermodynamic equilibrium. These simulations evidenced that at the conditions at which nucleation is expected to occur (which are those characterized by the formation of the GaX(NH₂)₂ species, as explained in the previous sections), the concentrations of the Ga₂NH(NH₂)₂XY species are 1 or 2 orders of magnitude higher with respect to those of the (Ga(NH₂)₂X)₂ dimers. This motivated the inclusion of the Ga₂NH(NH₂)₂XY species in the model and the proposal that they may be the reacting species leading to the formation of the first gas phase nuclei.

CONCLUSIONS

The main results of this work are twofold: the compilation of a thermodynamic database suitable to study the evolution of the gas phase composition as a function of the operative conditions during GaN MOVPE, and the proposal of a kinetic mechanism that may be used to describe the GaN gas phase reactivity when it is deposited from TMGa and ammonia.

The thermodynamic database was used to determine which are the main gas phase species that can be formed at different temperatures in the operative conditions at which high-quality GaN films are usually deposited (reduced pressure and V/III ratio of 500). It was found that the most stable Ga species is GaNH₂, which is predicted to be more stable than GaXYZ (X,Y,Z = CH₃, NH₂ or H), atomic Ga, or diatomic GaN. It is

thus proposed that GaNH₂ is the main GaN growth species. It would be quite important if this proposal could be proved experimentally, as such evidence is presently missing. Also, the thermodynamic analysis suggests that the precursors to the formation of GaN gas phase nuclei may be Ga species having the structure Ga₂NH(NH₂)₂XY. Two different nuclei structures were proposed and their thermodynamic stability was investigated. It was found that their equilibrium concentration rapidly increases with the decrease of the temperature. This suggests that, similarly to what happens for the nucleation and growth of soot, GaN powders may nucleate and growth in a well-defined temperature window.

The kinetic mechanism was constructed on the basis of the results of the thermodynamic study and exploiting sensitivity analysis on a 2D FEM model to identify the major reaction routes. The optimized mechanism consists of 54 reactions and includes 20 different species. Backward reactions are explicitly reported together with their rates when found to contribute significantly to the gas phase reactivity. Made exception for a few rate constants that were taken from the literature, all the rate constants included in the gas phase mechanism were here computed at a level of theory that is in general more advance with respect to what is reported in the literature for this system. The analysis of the gas phase reactivity was performed simulating a well-known MOVPE reactor. It was found that the conversion of Ga(CH₃)₃ to GaNH₂ occurs in several steps involving the gradual substitution of the Ga-CH₃ groups with the thermodynamically more stable Ga-NH₂ and Ga-H groups and is followed by several decomposition reactions. The kinetic analysis confirms the thermodynamic prediction that GaNH₂ is the most abundant Ga gas phase species that is present above the deposition surface.

The proposed kinetic mechanism contains also a set of reactions that lead to the formation of several Ga species that we propose to be the precursors to the first stable GaN nuclei, whose successive growth would lead to the formation of powders.

The capability of the proposed gas phase kinetic mechanism to properly describe the GaN growth kinetics as well as the nucleation of powders will be the subject of a successive work, which is currently in preparation.

ASSOCIATED CONTENT

Supporting Information

Thermodynamic data set, structures, vibrational frequencies, and inertia moments of wells and saddle points calculated at the M062X/6-311+G(d,p) level. The Supporting Information is available free of charge on the ACS Publications website.

AUTHOR INFORMATION

Corresponding Author

*Address: Dipartimento di Chimica, Materiali e Ingegneria chimica "Giulio Natta", Politecnico di Milano, via Mancinelli 7-20131 Milano, Italy. Tel: ++39-02-23993176; fax: +39-02-23993180; e-mail: carlo.cavallotti@polimi.it.

Notes

The authors declare no competing financial interest.

REFERENCES

(1) Watson, I. M. Metal organic vapour phase epitaxy of AlN, GaN, InN and their alloys: A key chemical technology for advanced device applications. *Coord. Chem. Rev.* **2013**, *257*, 2120–2141.

- (2) Mihopoulos, T. G.; Gupta, V.; Jensen, K. F. A reaction-transport model for AlGa_N MOVPE growth. *J. Cryst. Growth* **1998**, *195*, 733–739.
- (3) Dauelsberg, M.; Martin, C.; Protzmann, H.; Boyd, A. R.; Thrush, E. J.; Kaeppler, J.; Heuken, M.; Talalaev, R. A.; Yakovlev, E. V.; Kondratyev, A. V. Modeling and process design of III-nitride MOVPE at near-atmospheric pressure in close coupled showerhead and planetary reactors. *J. Cryst. Growth* **2007**, *298*, 418–424.
- (4) Dauelsberg, M.; Brien, D.; Poesche, R.; Schoen, O.; Yakovlev, E. V.; Segal, A. S.; Talalaev, R. A. Investigation of nitride MOVPE at high pressure and high growth rates in large production reactors by a combined modelling and experimental approach. *J. Cryst. Growth* **2011**, *315*, 224–228.
- (5) Sugiyama, M.; Yasukochi, S.; Shioda, T.; Shimogaki, Y.; Nakano, Y. Examination of intermediate species in GaN metal-organic vapor-phase epitaxy by selective-area growth. *Phys. Status Solidi C* **2010**, *7*, 2085–2087.
- (6) Tomita, Y.; Shioda, T.; Sugiyama, M.; Shimogaki, Y.; Nakano, Y. Role of vapor-phase diffusion in selective-area MOVPE of InGa_N/Ga_N MQWs. *J. Cryst. Growth* **2009**, *311*, 2813–2816.
- (7) Shioda, T.; Sugiyama, M.; Shimogaki, Y.; Nakano, Y. Selectivity enhancement by hydrogen addition in selective area metal-organic vapor phase epitaxy of GaN and InGa_N. *Phys. Status Solidi A* **2010**, *207*, 1375–1378.
- (8) Chen, C. H.; Liu, H.; Steigerwald, D.; Imler, W.; Kuo, C. P.; Craford, M. G.; Ludowise, M.; Lester, S.; Amano, J. A study of parasitic reactions between NH₃ and TMGa or TMAI. *J. Electron. Mater.* **1996**, *25*, 1004–1008.
- (9) Creighton, J. R.; Breiland, W. G.; Coltrin, M. E.; Pawlowski, R. P. Gas-phase nanoparticle formation during AlGa_N metalorganic vapor phase epitaxy. *Appl. Phys. Lett.* **2002**, *81*, 2626–2628.
- (10) Creighton, J. R.; Wang, G. T.; Breiland, W. G.; Coltrin, M. E. Nature of the parasitic chemistry during AlGa_N OMVPE. *J. Cryst. Growth* **2004**, *261*, 204–213.
- (11) Creighton, J. R.; Coltrin, M. E.; Figiel, J. J. Observations of gas-phase nanoparticles during InGa_N metal–organic chemical vapor deposition. *Appl. Phys. Lett.* **2008**, *93*, 171906.
- (12) Matsumoto, K.; Tokunaga, H.; Ubukata, A.; Ikenaga, K.; Fukuda, Y.; Tabuchi, T.; Kitamura, Y.; Koseki, S.; Yamaguchi, A.; Uematsu, K. High growth rate metal organic vapor phase epitaxy GaN. *J. Cryst. Growth* **2008**, *310*, 3950–3952.
- (13) Demchuk, A.; Porter, J.; Koplitz, B. Laser-assisted reactivity of triethylgallium or trimethylgallium with ammonia in constrained pulsed nozzle expansions. *J. Phys. Chem. A* **1998**, *102*, 8841–8846.
- (14) Bergmann, U.; Reimer, V.; Atakan, B. An experimental study of the reactions of trimethylgallium with ammonia and water over a wide temperature range. *Phys. Chem. Chem. Phys.* **1999**, *1*, 5593–5599.
- (15) Schafer, J.; Simons, A.; Wolfrum, J.; Fischer, R. A. Detection of gas-phase species in MOCVD of GaN using molecular beam quadrupole mass spectrometry. *Chem. Phys. Lett.* **2000**, *319*, 477–481.
- (16) Matsumoto, K.; Tachibana, A. Growth mechanism of atmospheric pressure MOVPE of GaN and its alloys: gas phase chemistry and its impact on reactor design. *J. Cryst. Growth* **2004**, *272*, 360–369.
- (17) Moscatelli, D.; Caccioppoli, P.; Cavallotti, C. Ab initio study of the gas phase nucleation mechanism of GaN. *Appl. Phys. Lett.* **2005**, *86*, 091106.
- (18) Hirako, A.; Kusakabe, K.; Ohkawa, K. Modeling of reaction pathways of GaN growth by metalorganic vapor-phase epitaxy using TMGa/NH₃/H₂ system: A computational fluid dynamics simulation study. *Jpn. J. Appl. Phys. I* **2005**, *44*, 874–879.
- (19) Sengupta, D.; Mazumder, S.; Kuykendall, W.; Lowry, S. A. Combined ab initio quantum chemistry and computational fluid dynamics calculations for prediction of gallium nitride growth. *J. Cryst. Growth* **2005**, *279*, 369–382.
- (20) Creighton, J. R.; Wang, G. T.; Coltrin, M. E. Fundamental chemistry and modeling of group-III nitride MOVPE. *J. Cryst. Growth* **2007**, *298*, 2–7.
- (21) Moscatelli, D.; Cavallotti, C. Theoretical investigation of the gas-phase kinetics active during the GaN MOVPE. *J. Phys. Chem. A* **2007**, *111*, 4620–4631.
- (22) Mondal, B.; Mandal, D.; Ghosh, D.; Das, A. K. Computational study on the growth of gallium nitride and a possible source of oxygen impurity. *J. Phys. Chem. A* **2010**, *114*, 5016–5025.
- (23) Ikeda, Y.; Ohmori, N.; Maida, N.; Senami, M.; Tachibana, A. Theoretical study of gallium nitride crystal growth reaction mechanism. *Jpn. J. Appl. Phys.* **2011**, *50*, 125601.
- (24) Tokoi, H.; Ohtake, A.; Tago, K.; Watanabe, K.; Mishima, T. Development of GaN growth reaction model using ab initio molecular orbital calculation and computational fluid dynamics of metalorganic vapor-phase epitaxy. *J. Electrochem. Soc.* **2012**, *159*, D270–D275.
- (25) Thon, A.; Keuch, T. F. High temperature adduct formation of trimethylgallium and ammonia. *Appl. Phys. Lett.* **1996**, *69*, 55–57.
- (26) Creighton, J. R.; Wang, G. T. Kinetics of metal organic–ammonia adduct decomposition: Implications for group-III nitride MOCVD. *J. Phys. Chem. A* **2005**, *109*, 10554–10562.
- (27) Wang, G. T.; Creighton, J. R. Complex formation of trimethylaluminum and trimethylgallium with ammonia: Evidence for a hydrogen-bonded adduct. *J. Phys. Chem. A* **2006**, *110*, 1094–1099.
- (28) Glockling, F.; Strafford, R. G. Electron impact studies on some group III metal alkyls. *J. Chem. Soc. A* **1971**, 1761–1763.
- (29) Nakamura, K.; Makino, O.; Tachibana, A.; Matsumoto, K. Quantum chemical study of parasitic reaction in III–V nitride semiconductor crystal growth. *J. Organomet. Chem.* **2000**, *611*, 514–524.
- (30) Timoshkin, A. Y.; Bettinger, H. F.; Schaefer, H. F. DFT Modeling of chemical vapor deposition of GaN from organogallium precursors. I. Thermodynamics of elimination reactions. *J. Phys. Chem. A* **2001**, *105*, 3240–3248.
- (31) Timoshkin, A. Y.; Bettinger, H. F.; Schaefer, H. F. DFT modeling of chemical vapor deposition of GaN from organogallium precursors. II. Structures of the oligomers and thermodynamics of the association processes. *J. Phys. Chem. A* **2001**, *105*, 3249–3258.
- (32) Schimid, R.; Basting, D. Gas phase chemistry in gallium nitride CVD: Theoretical determination of the arrhenius parameters for the first Ga–C bond homolysis of trimethylgallium. *J. Phys. Chem. A* **2005**, *109*, 2623–2630.
- (33) Fikri, M.; Makeich, A.; Rollmann, G.; Schulz, C.; Entel, P. Thermal decomposition of trimethylgallium Ga(CH₃)₃: A shock-tube study and first-principles calculations. *J. Phys. Chem. A* **2008**, *112*, 6330–6337.
- (34) Chase, M. W., Jr. NIST-JANAF Thermochemical Tables, Fourth Edition. *J. Phys. Chem. Ref. Data* **1998**, *9*, 1–1951.
- (35) Zhao, Y.; Truhlar, D. G. The M06 suite of density functionals for main group thermochemistry, thermochemical kinetics, non-covalent interactions, excited states, and transition elements: Two new functionals and systematic testing of four M06-class functionals and 12 other functionals. *Theor. Chem. Acc.* **2008**, *120*, 215–241.
- (36) Derudi, M.; Polino, D.; Cavallotti, C. Toluene and benzyl decomposition mechanisms: Elementary reactions and kinetic simulations. *Phys. Chem. Chem. Phys.* **2011**, *13*, 21308–21318.
- (37) Polino, D.; Cavallotti, C. Fulvenallene decomposition kinetics. *J. Phys. Chem. A* **2011**, *115*, 10281–10289.
- (38) Polino, D.; Famulari, A.; Cavallotti, C. Analysis of the reactivity on the C₇H₆ potential energy surface. *J. Phys. Chem. A* **2011**, *115*, 7928–7936.
- (39) Wood, G. P. F.; Radom, L.; Petersson, G. A.; Barnes, E. C.; Frisch, M. J.; Montgomery, J. A., Jr. A restricted-open-shell complete-basis-set model chemistry. *J. Chem. Phys.* **2006**, *125*, 094106.
- (40) Raghavachari, K.; Trucks, G. W.; Pople, J. A.; Headgordon, M. A 5th-order perturbation comparison of electron correlation theories. *Chem. Phys. Lett.* **1989**, *157*, 479–483.
- (41) Fascella, S.; Cavallotti, C.; Rota, R.; Carrà, S. Quantum chemistry investigation of key reactions involved in the formation of naphthalene and indene. *J. Phys. Chem. A* **2004**, *108*, 3829–3843.

- (42) Fascella, S.; Cavallotti, C.; Rota, R.; Carra, S. The peculiar kinetics of the reaction between acetylene and the cyclopentadienyl radical. *J. Phys. Chem. A* **2005**, *109*, 7546–7557.
- (43) Frisch, M. J.; Trucks, G. W.; Schlegel, H. B.; Scuseria, G. E.; Robb, M. A.; Cheeseman, J. R.; Scalmani, G.; Barone, V.; Mennucci, B.; Petersson, G. A. et al. *Gaussian 09*, revision A.1; Gaussian, Inc.: Wallingford, CT, 2009.
- (44) Banerjee, S.; Cole, J. V.; Jensen, K. F. Nonlinear model reduction strategies for rapid thermal processing systems. *IEEE Trans. Semicond. Manuf.* **1998**, *11*, 266–275.
- (45) Merchant, T. P.; Cole, J. V.; Knutson, K. L.; Hebb, J. P.; Jensen, K. F. A systematic approach to simulating rapid thermal processing systems. *J. Electrochem. Soc.* **1996**, *143*, 2035–2043.
- (46) Jensen, K. F.; Mihopoulos, T. G.; Rodgers, S.; Simka, H. CVD simulations on multiple length scales. *Proc. Thirteenth Int. Conf. CVD Electrochem. Soc.* **1996**, PV 96–5, 67–74.
- (47) Barbato, A.; Cavallotti, C. Challenges of introducing quantitative elementary reactions in multiscale models of thin film deposition. *Phys. Status Solidi B* **2010**, *247*, 2127–2146.
- (48) Cavallotti, C.; Nemirovskaya, M.; Jensen, K. F. A multiscale study of the selective MOVPE of $\text{Al}_x\text{Ga}_{1-x}\text{As}$ in the presence of HCl. *J. Cryst. Growth* **2003**, *248*, 411–416.
- (49) Cavallotti, C.; Lengyel, L.; Nemirovskaya, M.; Jensen, K. F. A computational study of gas-phase and surface reactions in deposition and etching of GaAs and AlAs in the presence of HCl. *J. Cryst. Growth* **2003**, *248*, 411–416.
- (50) Cavallotti, C.; Pantano, E.; Veneroni, A.; Masi, M. Multiscale simulation of silicon film growth. *Cryst. Res. Technol.* **2005**, *40*, 958–963.
- (51) Cavallotti, C.; Gupta, V.; Sieber, C.; Jensen, K. F. Dissociation reactions of $\text{Cu}^{\text{I}}(\text{hfac})\text{L}$ compounds relevant to the chemical vapor deposition of copper. *Phys. Chem. Chem. Phys.* **2003**, *5*, 2818–2827.
- (52) Naji, O.; Zhang, J.; Kaneko, T.; Jones, T. S.; Neave, J. H.; Joyce, B. A. A detailed time of flight study of the cracking pattern of trimethylgallium; Implications for MOMBE growth. *J. Cryst. Growth* **1996**, *164*, 58–65.
- (53) Himmel, H.-J.; Downs, A. J.; Greene, T. M. Thermal and photochemical reactions of aluminum, gallium, and indium atoms (M) in the presence of ammonia: Generation and characterization of the species $\text{M}\cdot\text{NH}_3$, HMNH_2 , MNH_2 , and H_2MNH_2 . *J. Am. Chem. Soc.* **2000**, *122*, 9793–9807.
- (54) Yu, Y. X.; Li, S. M.; Xu, Z. F.; Li, Z. S.; Sun, C. C. An ab initio study on the reaction $\text{NH}_2 + \text{CH}_4 \rightarrow \text{NH}_3 + \text{CH}_3$. *Chem. Phys. Lett.* **1998**, *296*, 131–136.
- (55) Mebel, A. M.; Lin, M. C. Prediction of absolute rate constants for the reactions of NH_2 with alkanes from ab initio G2M/TSST calculations. *J. Phys. Chem. A* **1999**, *103*, 2088–2096.
- (56) Baulch, D. L.; Cobos, C. J.; Cox, R. A.; Esser, C.; Frank, P.; Just, T.; Kerr, J. A.; Pilling, M. J.; Troe, J.; Walker, R. W.; Warnatz, J. Evaluated kinetic data for combustion modelling. *J. Phys. Chem. Ref. Data* **1992**, *21*, 411–734.
- (57) Corchado, J. C.; Espinosa-Garcia, J. Analytical potential energy surface for the $\text{NH}_3 + \text{H} \leftrightarrow \text{NH}_2 + \text{H}_2$ reaction: Application of variational transition-state theory and analysis of the equilibrium constants and kinetic isotope effects using curvilinear and rectilinear coordinates. *J. Chem. Phys.* **1997**, *106*, 4013–4021.
- (58) Smith, G. P.; Golden, D. M.; Frenklach, M.; Moriarty, M. W.; Eiteneer, B.; Goldenberg, M.; Bowman, T.; Hanson, R. K.; Song, S.; Gardiner et al. Gri-Mech 3.0. http://www.me.berkeley.edu/gri_mech/, accessed Dec 2014.
- (59) Jegier, J. A.; McKernan, S.; Gladfelter, W. L. Solution chemistry of cyclotrigallazane: Supercritical ammonia and Lewis base catalyzed dehydrogenation to produce poly(imidogallane). *Inorg. Chem.* **1999**, *38*, 2726–2733.
- (60) Reid, R. C.; Prausnitz, J. M.; Sherwood, T. K. *The Properties of Gases and Liquids*; Mc Graw-Hill: New York, 1977.